World Journal of Engineering Research and Technology
WJERT
www.wjert.org
SJIF Impact Factor: 5.218

ANALYSIS OF EARTH SLOPES SUBJECTED TO CHANGE IN WATER CONTENT USING CENTRIFUGE MODELLING

Endalkachew Mergia Anbese*[1] and Prof. Ashish Juneja[2]

[1]MSc, Department of Civil Engineering, Ambo University, Ambo, Ethiopia.
[2](Ph. D.) Department of Civil Engineering, Indian Institute of Technology Bombay, Powai, Mumbai, India.

Article Received on 20/12/2017 **Article Revised on 10/01/2018** **Article Accepted on 31/01/2018**

***Corresponding Author**
Endalkachew Mergia Anbese
MSc, Department of Civil Engineering, Ambo University, Ambo, Ethiopia.

ABSTRACT

This paper discusses the results of soil slope stability using a small beam centrifuge. Model slopes were prepared using residual soils, compacted at dry state. Properties of the soil used in this study are discussed first. The slopes were prepared by tamping the soil in a small, strong box made of perspex. A perforated water tank was placed behind the slope to permit the seepage of water through the soil. The provision was made to collect the water above the base plate. The slope angle was varied from 60 to 75°, and the slope was examined in different water content conditions. Digital images were captured at fixed intervals and analyzed. The result from the parametric studies shows the quantitative data points of Stability number at different gravity scale. It was observed that the relationships obtained in this study, are comparable to Taylor's Stability number.

KEYWORDS: Slope stability, Centrifuge modeling, Taylor's Stability number.

INTRODUCTION

Cross-Section of an embankment is usually trapezoidal and comprises of slope structure. To calculate its stability, it is necessary to understand its side slope stability. The factors which affect the side slope stability include the physical properties of the soil, external loads and water infiltration (Terzaghi, 1950). Its vital work is to support entire structure and the loads. Support to the embankment is given by its slope filled soil. Slopes are characterized by non-uniform stress field (Picarelli 2000). Bishop's modified method, Janbu's generalized

procedure of slices and force equilibrium are the few methods which are used in the stability analysis. Failures in unsaturated residual soil slopes occur during the wet season. During this period, the shear strength is reduced and the pressure applied by the soil is increased. Shimada et al. (1995), Fredlund and Rahardjo (1994), Oeberg (1995) and Alonso et al. (1995) studied the effect of infiltration on the stability of dry slopes.

Residual soils collected from the west coast of India were used in this study. These soils have traditionally been formed by chemical weathering of laterites, and basalt rocks bedded deep below the ground surface. Stability of the embankment made of the above soils was modeled using a small beam centrifuge. A prototype physical model similar to the one developed by Bucky (1931) was used at a reduced scale. Centrifuge modeling helps to draw a relationship between stability number and angle of slope. The failure event in nature cannot be stimulated on the laboratory floor at 1g. Reduce scale model is relatively inexpensive and favorable process to understand changes in stress and soil deformation in the prototype. In the model, the linear dimensions of the embankment were reduced by n-g, where n is the centrifuge acceleration, and g is the earth's gravity. By centrifuge scaling laws, n-times greater than model was achieved by increasing the acceleration by n.

Experimental Setup

The analysis of slope stability was performed using centrifuge model. Before the generation of the physical model, properties of soil were investigated since these results were considered to be helpful in further analysis. The following procedural method is outlined to check the stability of slopes.

Physical Properties of Residual Soil

Following properties were evaluated

Water content by oven drying method.

The specific gravity of soil by density bottle.

Particle size distribution by mechanical sieving.

Particle size distribution less than 75μm by hydrometer.

Atterberg and shrinkage limit.

Compaction characteristics of soil by compaction test.

Table 1: Material properties of residual soil.

Soil Properties	Magnitude
Natural Moisture Content (%)	21
Specific Gravity	2.75
Liquid Limit (&)	49
Plastic Limit (%)	29
Shrinkage Limit (%)	19.7
Plasticity Index (%)	20
Soil Classification	ML
Maximum Dry Unit weight (kN/m^3)	14.5
Optimum Moisture Content (%)	24
UCS (kPa)	35.6

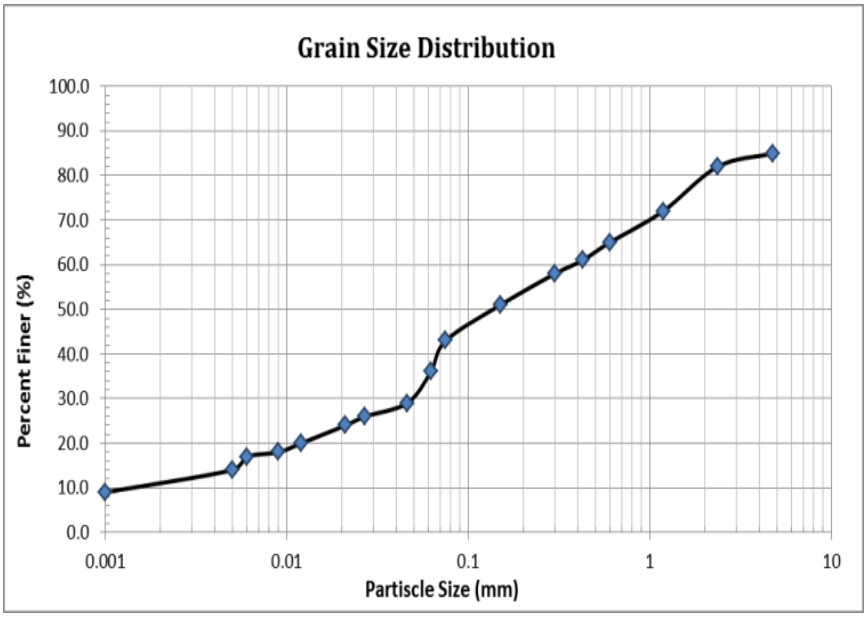

Fig. 1: Particle size distribution curve of soil.

SEM (Scanning Electron Microscopy)

Scanning Electron Microscope is helpful in developing electron digital images. The images analysis was done at different magnifications Fig. 2 at 800 times, Fig. 3 at 5000 times and Fig. 4 at 10000 times. All of these images were captured at CRNTS IIT Bombay.

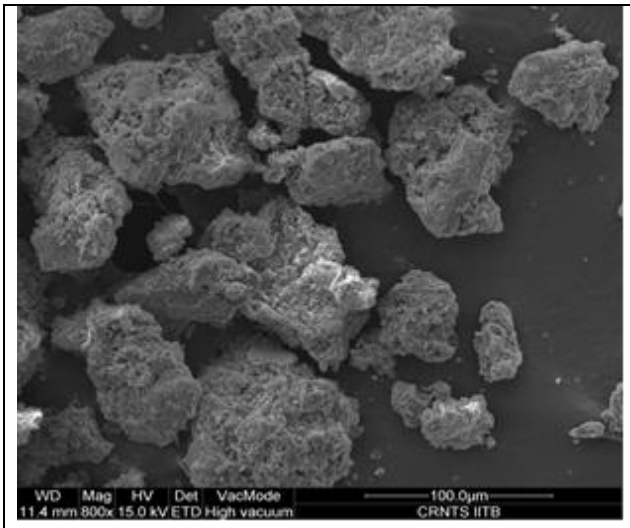

Fig. 2: SEM images at 800 times magnification.

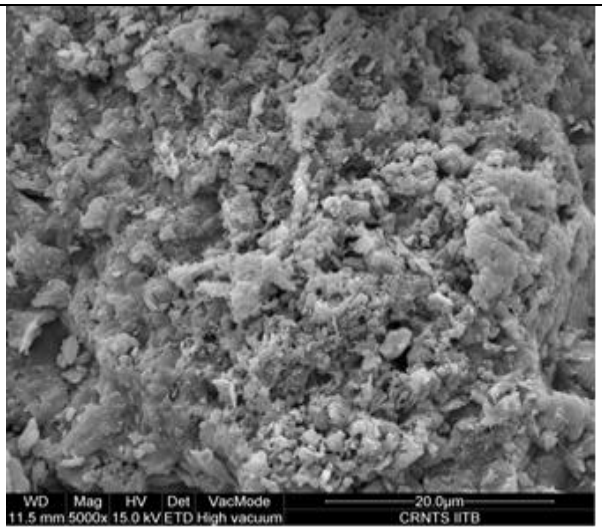

Fig. 3. SEM images at 5000 times magnification.

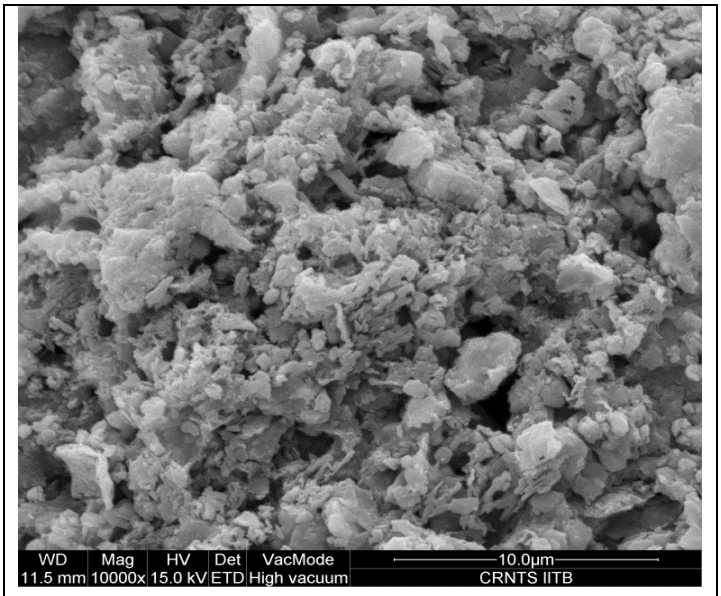

Fig. 4: SEM images at 10000 times magnification.

EDAX Energy-dispersive X-ray spectroscopy

It is the analytical process of obtaining chemical composition of the sample. The analysis shows the peak of each element.

Four primary components of EDAX are:

1. X-ray beam
2. X-ray detector
3. Pulse processor
4. The Analyzer

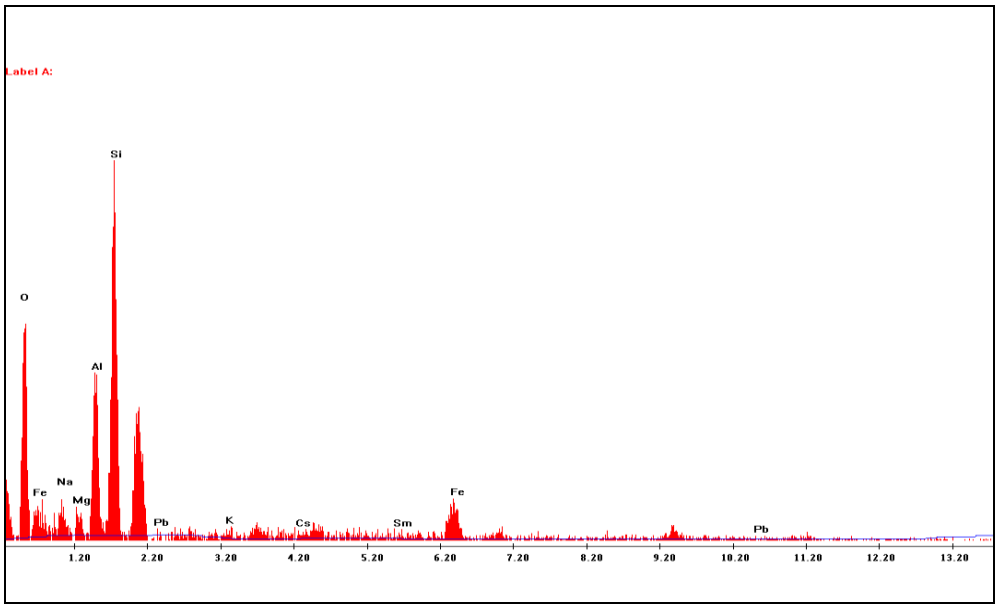

Fig. 5: EDAX analysis.

Soil Strength

It was necessary to obtain the undrained shear strength of soil. The procedure was adopted for calculating strength; a series of UU Triaxial test and UCS over dry soil were performed. In UU Triaxial test, the degree of saturation was increased from 0.2 to 1 and decrement in undrained shear strength was obtained. For each test, the plot shows the notable effect of water content on the undrained strength of soil. By this, an exponential relationship was fitted over the acquired data points.

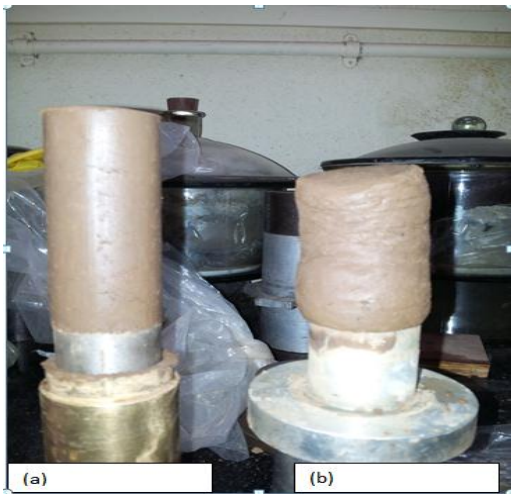

Fig. 6: UU Triaxial Test (a) before test (b) after test.

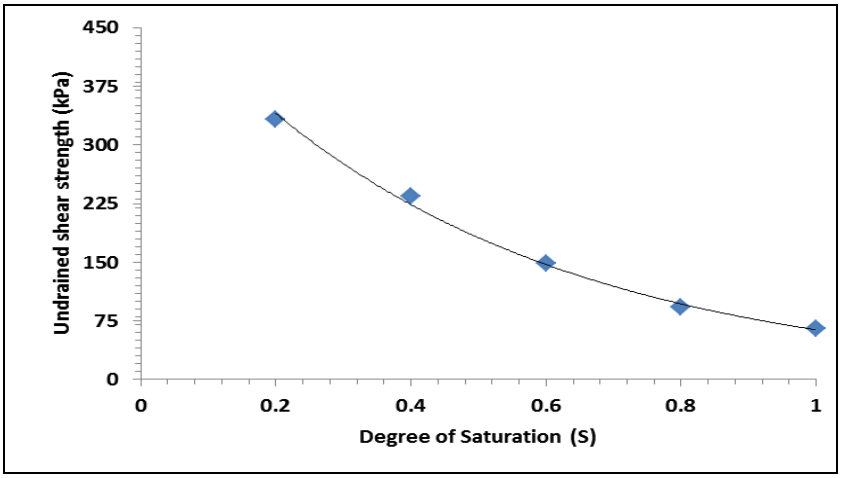

Fig. 7: Variation of undrained shear strength, S_u with degree of saturation.

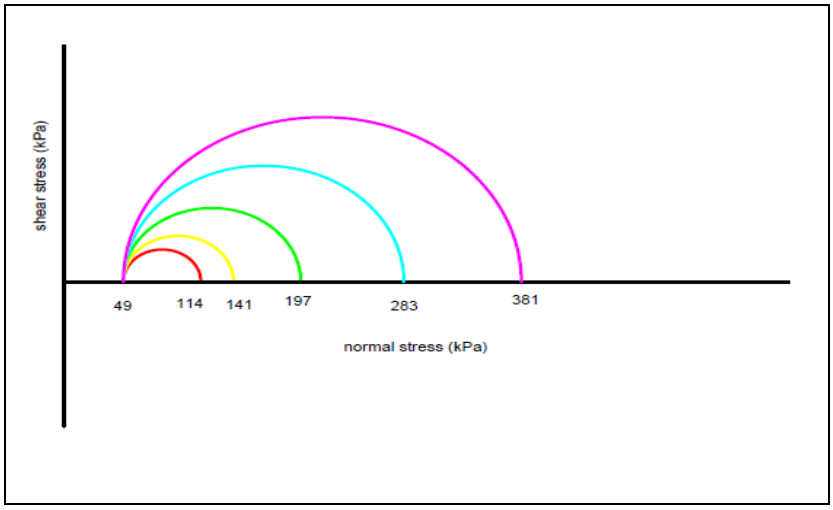

Fig. 8: Mohr Circle for the UU Triaxial Test.

Physical Modelling Of The Centrifuge

A full-scale physical model of the centrifuge was given by Bucky (1931). It helps to scaled-down models and upholds the stress states required for developing appropriate soil properties. The combination of analytical limit equilibrium and experimental centrifuge modeling results helps to probe the performance of slopes. Based on dimensions analysis, the centrifugal model test was summarized by Fuglsang and Ovesen (1986). The relation between model and prototype is given by scaling law. It is defined that the gravity scale $N = a/g$, where '*a*' is the centrifugal acceleration, and '*g*' is the gravity acceleration. To create prototype slope for centrifuge box "scaling small-scale model (SSSM)" is adopted. Acceleration of SSSM was *N* times of the gravity acceleration, generating the same stresses in centrifugal model and prototype.

The modeling was done performed on balance beam small centrifuge having arm radius was 0.49 m. When driving unit stimulates the centrifugal movement, the angular velocity attained stimulates a particular Gravity Scale (N) called Scaling Factor. The scaling factor achieved helps to calculate the critical height of prototype.

The centrifuge has salient features:

1. Driving Unit
2. Speed Regulator
3. Digi-strobe

Driving Unit consists of a universal 0.5HP motor, with a swinging bucket on both sides of the arm. The maximum payload can be taken 0.02 kN. Speed Regulator helps to initiate the in-flight condition and helps to achieve the failure of slopes. Digi-Strobe called stroboscope helps to appear cyclic moving objects in a slow-moving string. It's as synchronized as the sample arrives in front of a transparent screen of the lid, the light flashes and makes the box appear. It yields 50-50000 flashes per min.

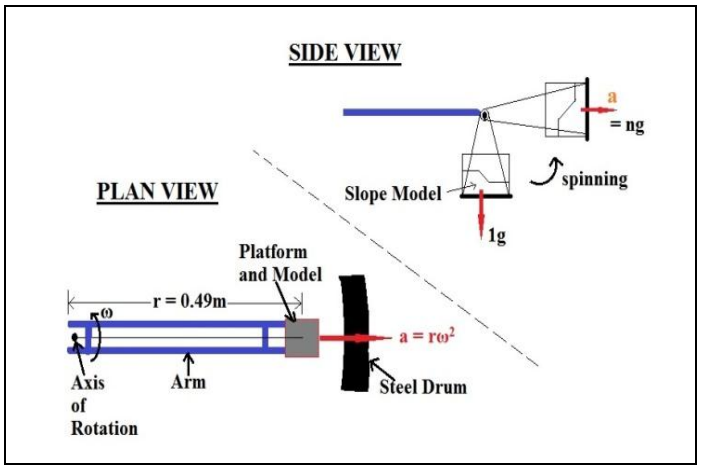

Fig. 9: Plan and Side View of Balance Beam Centrifuge.

Test Setup for ng Physical Modelling

Physical modeling includes a strong box of Perspex material, containing bed slopes with seepage tank. The internal dimensions of tank were160mm x 1130m x 60mm. Perforated Seepage tank attached adjacent the tank. Holes were arranged in a single central line with gauge distance of 2mm and 1.5mm diameter. Seepage flow was controlled by applying geotextile sheet on the inner face of the tank. Sheet makes water to flow all around the face of tank uniformly.

Preparation of ng Model Slope

The small-scale model of the slope was housed in a strong box. The slope model consisted of a homogeneous residual soil slope. The different geometrical dimensional slope was prepared as listed in Table 2. The analysis includes varying seepage conditions, by perforated seepage tank, placed behind the slope built. For generating in-built delight, condition slope was prepared, and the corresponding payload was measured.

Test Program for the Small-Scale Model Test

The following experimental program focused mainly on the performance of the slope model when the seepage was performed. The primary purpose of the experiment was to probe the critical height of slope at different slope angles. The modes of failure of slopes were seen in on toe, slope surface, i.e., due to erosion, hairline cracks on slope surface.

Before preparing soil slope model, the weight of soil was calculated by unit weight of the sample and the volume of the desired slope. The soil was tamped in different layers. Freeboard of minimum 1mm was provided. The cuboidal soil block was prepared, and cutting was performed according to the desired marked slope. As the sample was dry, the sample was handled and trimmed gently.

Test Conditions Over Dry Soil

The following test programme was adopted in the study.

1. Dry soil slope was prepared and was stimulated without seepage. The slope was checked till failure at every constant interval of angular velocity.
2. Dry soil slope was prepared and was stimulated without seepage. The slope was checked directly to the failing angular velocity.
3. Dry soil slope was prepared and was stimulated with seepage. The slope was checked till failure at every constant interval of angular velocity.
4. Dry soil slope was prepared and was stimulated with seepage. The slope was checked directly to the failing angular velocity.

Table-2.

Test no.	Slope angle (degree)	Model height (m)	Base Length(m)
1	60	0.08	0.46
2	65	0.08	0.37
3	70	0.08	0.29
4	75	0.08	0.21

CONDITION 1

After the sample preparation for each slope counterbalance was measured, both were placed in-flight setup. This was how the in-flight condition was built up, and the test was performed. In this case, the centrifuge was operated at incremental angular velocity. At every constant increment of angular velocity, the centrifuge was slowed down. The box was removed, and condition of the slope was checked. Digital images were captured immediately after the removal of strong box. The box was then replaced in the centrifuge for the higher g level. The increment process was continued until the slope movement was recorded in the digital images.

(a) Slope angle-60°

(c) Slope angle-70°

(b) Slope angle-65°

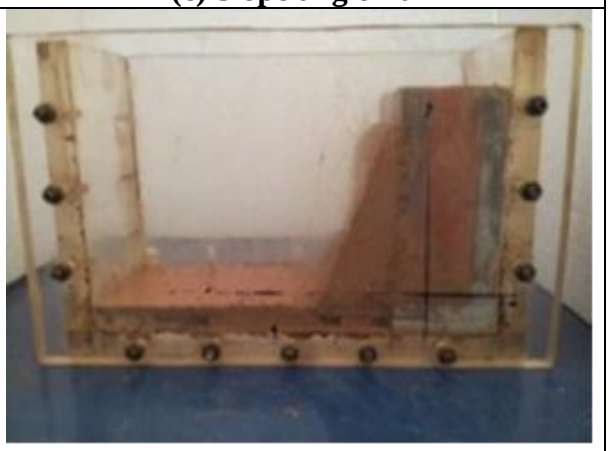

(d) Slope angle-75°

Figs. 10: a-d Slope condition for the Dry sample, without seepage and check of failure at every constant interval of angular velocity.

CONDITION 2

The test conditions are similar to above condition, but in this case, the centrifuge was operated to directly to near the failing angular velocity. To check the exact failing point Stroboscope is placed over the transparent screen of the centrifuge. The stroboscope is

electronic devices which emits rapid flashes of light as the sample passes over it. This was helpful to view a sample.

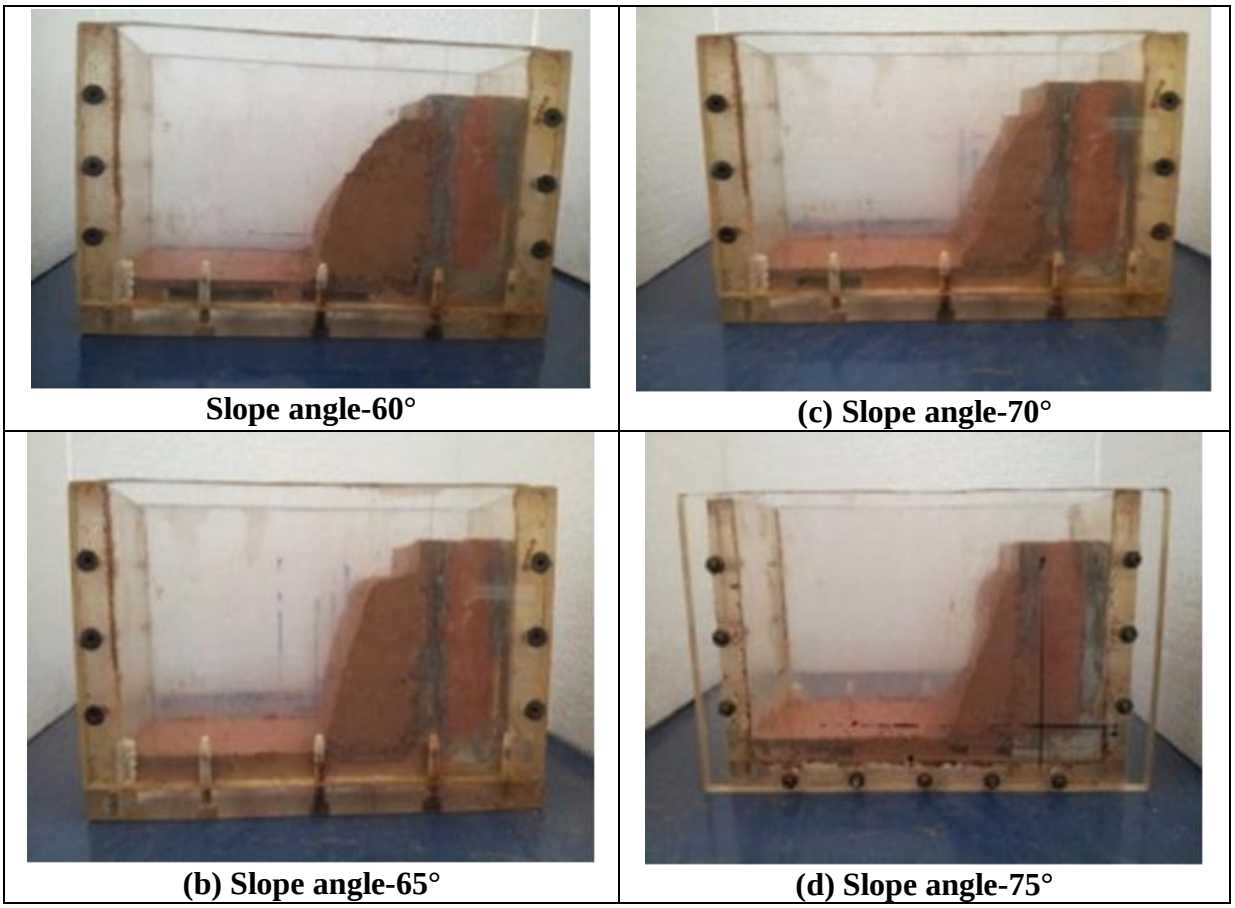

Slope angle-60° **(c) Slope angle-70°**

(b) Slope angle-65° **(d) Slope angle-75°**

Fig. 11: a-d. Dry sample, without seepage and check of failure to direct near about failing angular velocity.

CONDITION 3

Centrifuge modeling is helpful in check of the different condition of slopes. In this condition, slopes were designed at different angles and condition of controlled seepage was introduced. Seepage was equally distributed along the face by use geotextile. Slopes were placed in centrifuge modeling and same procedure of stopping and removing of the box was done. In this, seepage movement was also checked. As the angular velocity increase, water starts its movement from toe to crest side of the slope. Every constant interval of angular velocity images was produced and failing angular velocity was recorded.

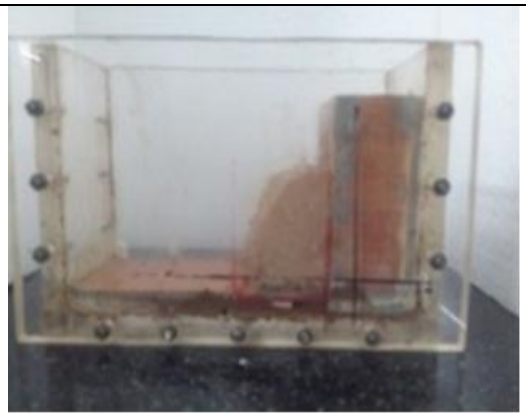

Slope angle-60°

(c) Slope angle-70°

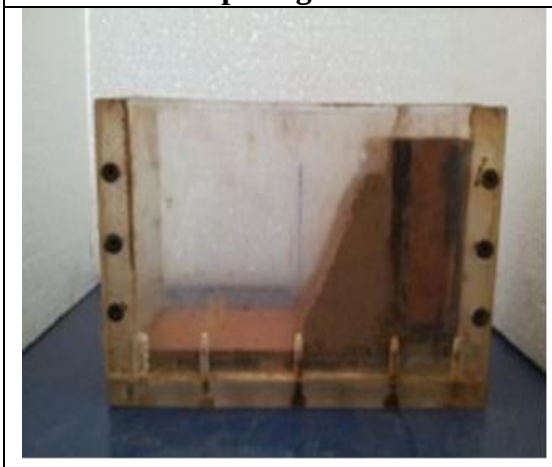

(b) Slope angle-65°

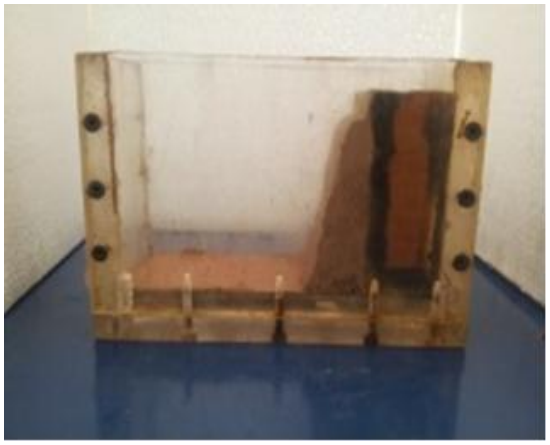

(d) Slope angle-75°

Fig. 12. a-d Dry sample, with seepage and check of failure at every constant interval of angular velocity.

CONDITION 4

After checking the centrifuge at every incremental angular velocity for activated seepage conditions, in this condition, the direct increment of angular velocity to failing value was done. This process consists of image processing at starting and final time of setup.

(a) Slope angle-60°

(c) Slope angle-70°

(b) Slope angle-65°

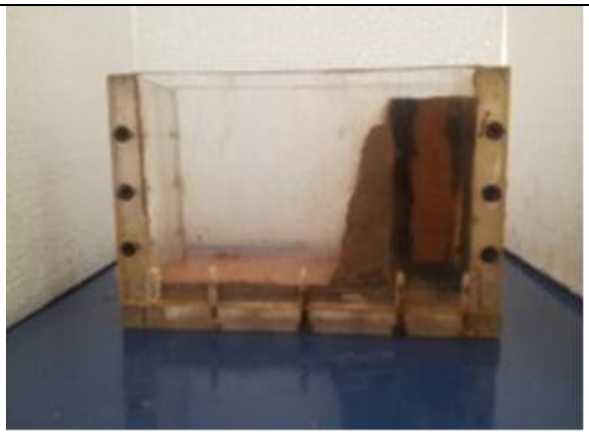

(d) Slope angle-75°

Fig. 13: a-d. Dry sample, with seepage and check of failure to direct nearabout failing angular velocity.

Condition 4 comprises of incremental loading and unloading. At every constant interval of angular velocity, the condition of the slope was checked. Fig. 14 shows the failure points at the direct incremental condition. The graph shows a variation of stability number along different slope angles. The setup compares two conditions, with seepage and other without seepage.

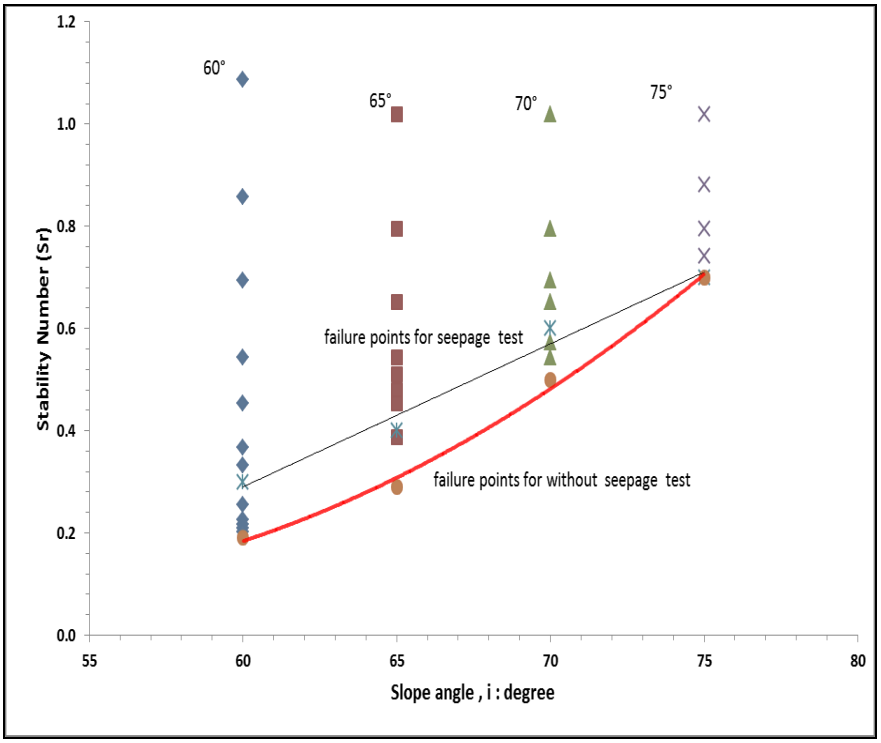

Fig. 14: Comparing Incremental loading-unloading conditions with and without seepage.

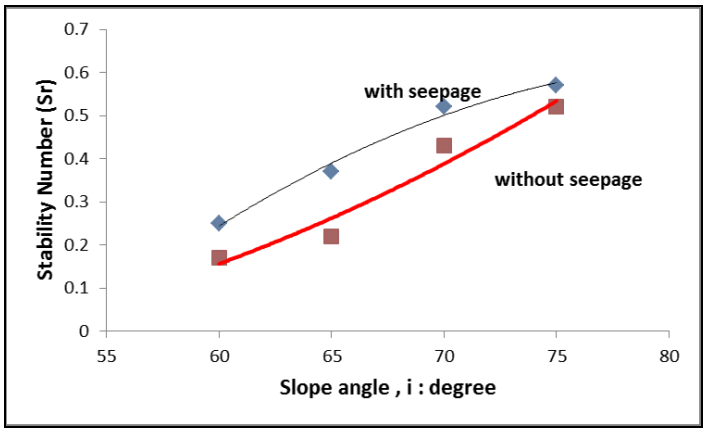

Fig. 15: Comparison of direct centrifuge modeling with and without seepage.

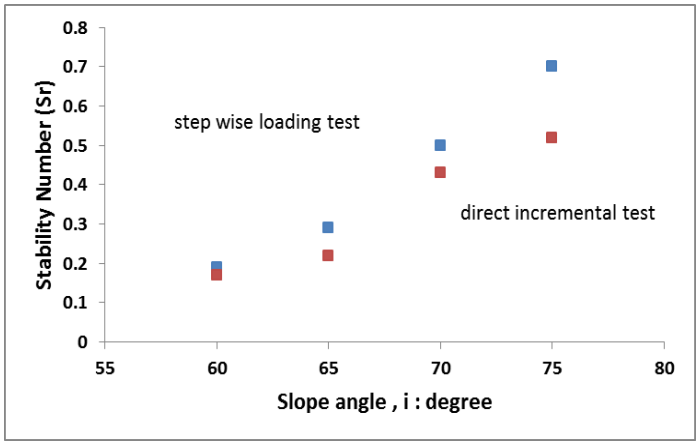

Fig. 16: Comparison of without seepage centrifuge modeling.

Figure 15 shows the comparison between direct incremental and loading-unloading incremental condition. In this condition, seepage condition wasn't stimulated. The figure also shows the variation of stability number along different slope angles.

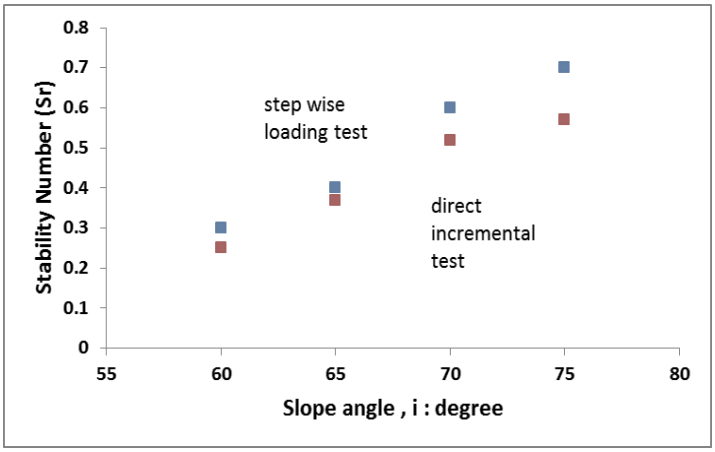

Fig. 17: Comparison of with seepage centrifuge modeling.

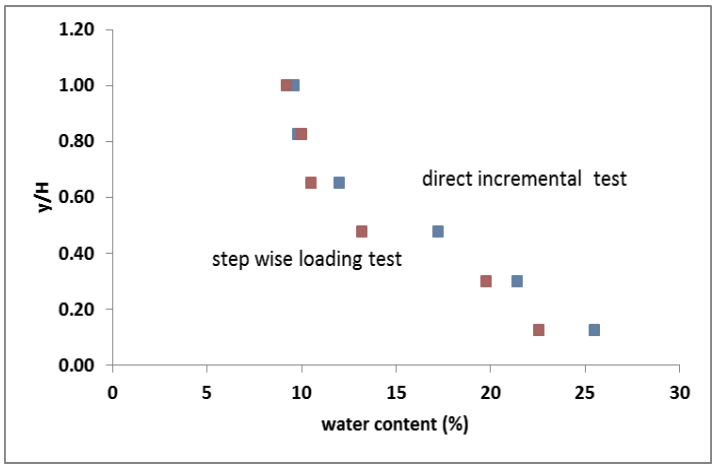

Fig. 18: Comparison between Increment and direct test at slope angle 60°.

Figure 17 shows the comparison between direct incremental and loading-unloading incremental condition. In this comparison, seepage was stimulated. The graph shows a variation of stability number along different slope angles.

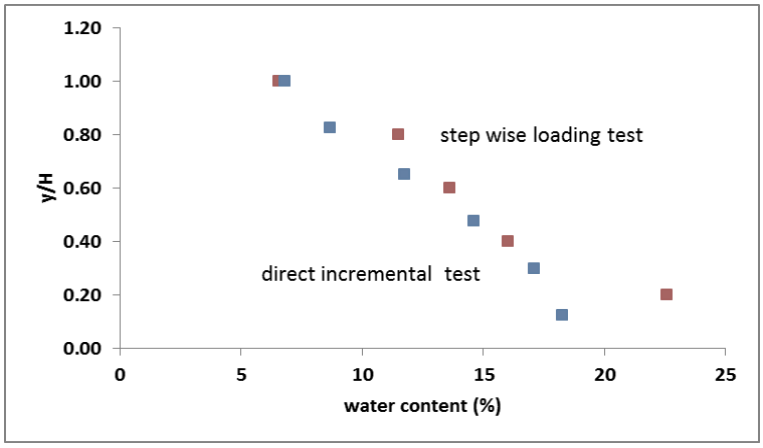

Fig. 19: Comparison between Increment and direct test at slope angle 65°.

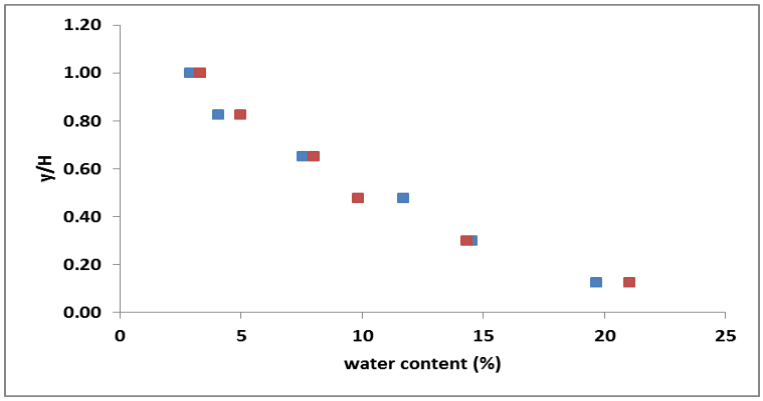

Fig. 20: Comparison between Increment and direct test at slope angle 70°.

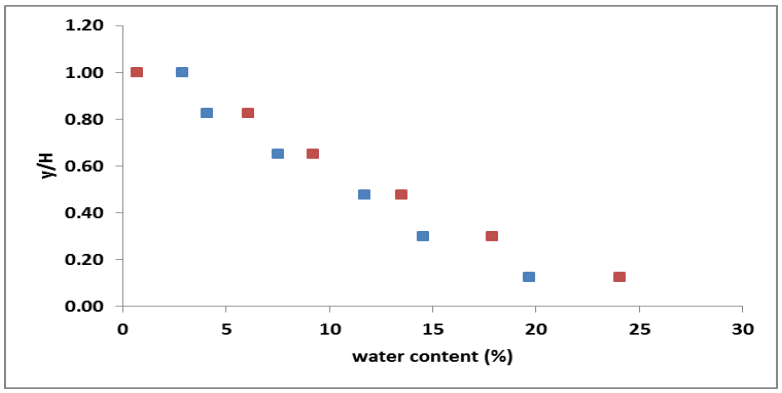

Fig. 21: Comparison between Increment and direct test at slope angle 75°.

Figures 18 to 20 show the water content along the slope height. Water content was measured and compared to direct incremental and loading-unloading incremental angular. The test was performed at 60°, 65°, 70° and 75 ° angles at the dry compacted soil. Proposed model Height of soil slope was 80 mm. Graphs depict that water content varies along the height from w=3 % at top and w= 24% at the bottom portion. So, we can expect a variation of apparent cohesion along the height of model. For peak strength, UU triaxial and unconfined compression strength Test was performed. Other case included for the study of variation of water content along the slope height was compacted slope at 65° at a different model height at OMC.

Table 3:

Test no.	Slope angle (degree)	Model height (m)	Base Length(m)
1	65	0.40	0.18
2	65	0.45	0.21
3	65	0.50	0.23
4	65	0.55	0.25
5	65	0.70	0.32
6	65	0.75	0.35

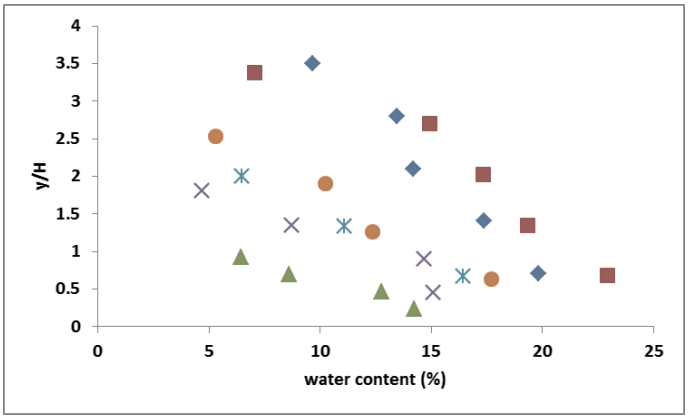

Fig. 22: Variation of water content along slope height in OMC soil condition.

Water levels in different conditions are to be checked. In the following experimental setup, soil slopes were built on Optimum Moisture Content with enabled seepage condition.

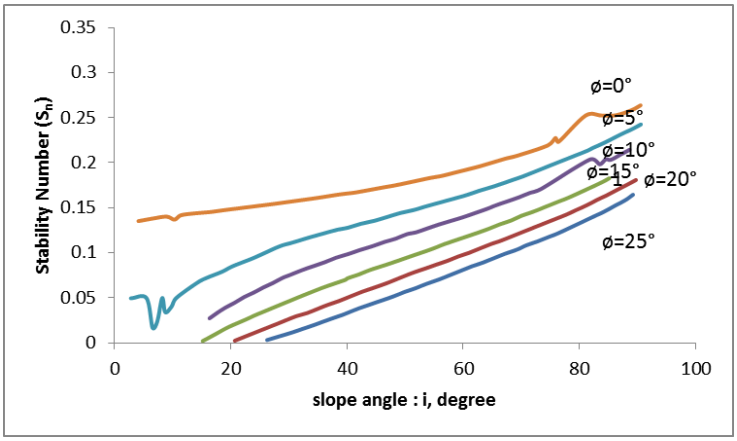

Fig. 23: Taylor's stability chart (1948).

DISCUSSION

Various tests on different soil slopes were performed. Test results were compared with different seepage condition. Table 2 comprises the geometry of slopes formed for test on dry soil slopes. Both conditions, with and without seepage were performed on prepared test slopes. Fig. 11. shows the relations between with and without seepage condition in incremental loading and unloading condition. At every stoppage condition of the slope was examined and stability number was computed.

$$Sn = \frac{Cu}{F * \gamma * H} \qquad (1)$$

Where: F is the safety factor equal to unity.

Figure 13 shows the relations between with and without seepage condition in incremental direct loading condition. Slopes were examined directly at failure angular velocity, and stability number was evaluated using Eq. 1. From the above test performed Fig. 15 and Fig. 16 comprises without and with seepage in incremental loading-unloading condition respectively. In the seepage analysis, water content along height was checked. Figs. 16-19 shows a comparison of direct and incremental loading-unloading condition at different slope angles. Water content varies from top to bottom from 3% to 24%.

Considering phase 2 in which slope was prepared at 65° at Optimum Moisture Content. 6 model test series with different slope height were formulated. Water content along the slope

height was calculated at every constant interval. Fig. 21 shows the water content. In every slope, soil at top crest has low water content (1 to 3%) whereas soil at toe has water content varies from (14 to 23%).

CONCLUSION

Residual soil with its high permeability and silty clay shows unusual characteristics. The water flows in the soil very easily and causes many variations along the slope height. In every test, slopes water content along the height decreases from apex to bottom. Fig. 16-19 and Fig. 20 showed variation of water along the slope height in different slope conditions. In either of the case, water content at toe was less than Optimum Moisture Content (S<1). These findings implied the following:

- In case of OMC prepared slope, as the slope height increases, saturation at toe side has reached up to 100%. In case of dry soil slopes, failing angular velocity is more for without seepage condition in both direct and incremental loading-unloading condition.
- The undrained shear strength of residual soil has reduced with an increase in saturation from 0.20 to 1.0.

REFERENCE

1. Tohari, A.Nishigaki, M., and Komatsu.M. "Laboratory Rainfall-Induced Slope Failure with Moisture Content Measurement," Journal of Geotechnical and Geo-Environmental Engineering ASCE, 2007; 133: 575-587.
2. Juneja, A., Chatterjee, D. and Kumar, R. "Embankment failure in residual soils at Nivsar, Ratnagiri", International Journal of Geo-Engineering Case Histories, 2012; 2(3): 229-251.
3. Vishwanathan, B.V.S and Mahajan, R. R. "Centrifuge model tests on geotextile-reinforced slopes," Geosynthetics International, 2007; 14(6).
4. Grkceoglu, C and Aksoy, H. “Landslide susceptibility mapping of the slopes in the residual soils of the Mengen region (Turkey) by deterministic stability analyses and image processing techniques," Engineering Geology 1996; 44: 147-161.
5. Ng, C.W.W. and Shi. Q. “A numerical investigation of the stability of unsaturated soil slopes subjected to transient seepage," Computers and Geotechnics, 1997; 22(1): 1-28.
6. Cai, F. and Ugai, K. “Numerical Analysis of rainfall effects on slope stability," International Journal of Geomechanics, 2004; 4(2): 69-78.
7. Fredlund, D.G. and Rahardjo, H. Soil mechanics for unsaturated soils. John Wiley & Sons, New York, 1993.

8. Ling; H. I., Wu; M.H., Leshchinsky, d., and Leshchinsky, B. “Centrifuge Modelling of Slope Instability," Journal of Geotechnical and Geo-Environmental Engineering, ASCE, 2009; 135: 758-767.
9. Kim, J. Jeong, S. Park, S. and Sharma, J. "Influence of rainfall-induced wetting on the stability of slopes in weathered soils," Engineering Geology, 2004; 75: 251–262.
10. Tan, L.Y. Lee and Sivadass, T. "Parametric study of residual soil slope stability," ICCBT, 2008; E-04: 33-42.